

Crystallization kinetics of Zr-rich $\text{Fe}_x\text{Zr}_{100-x}$ ($20 \leq x \leq 40$) metallic glasses

MAKOTO MATSUURA

Miyagi National College of Technology, Nodayama Natori Miyagi 981-12, Japan

The crystallization kinetics of the melt-spun Fe–Zr metallic glasses in the iron-rich region has been investigated by means of DSC and X-ray diffraction. The crystallization mode changes with iron concentration. In the lower iron region, $20 \leq x \leq 25$, the $\text{Fe}_x\text{Zr}_{100-x}$ glasses crystallize into ω -Zr and Ti_2Ni -type FeZr_2 with an accompanying sharp and large exotherm at the first crystallization step and immediately after this step, they transform into orthorhombic FeZr_3 . On the other hand, the alloys with $35 \leq x \leq 40$ exhibit a gradual exotherm which initiates from a temperature far below the definite crystallization temperature (T_x). The Fe–Zr metallic glasses in this concentration region crystallize polymorphously into the oxygen-stabilized Ti_2Ni -type FeZr_2 with accompanying relatively small and composite exotherms. The annealing at a temperature where the gradual exotherm occurs for the alloys with $30 \leq x \leq 40$ does not cause any changes of X-ray halo pattern but results in the reduction of the heat of exotherm due to the crystallization.

1. Introduction

Numerous works have been published concerning the crystallization kinetics of the transition metal–metalloid glasses. But the easy glass formation range for these alloys is limited to the concentration around the eutectic point. On the other hand, the metal–metal glasses such as Zr–(Cu, Fe, Co and Ni) can be vitrified by means of melt-spinning over a wide concentration range even in which a stable crystalline compound is formed. Therefore, zirconium based metal–metal glasses have the advantage that we can study the concentration effects on the crystallization kinetics over a wide range.

Although many works have been published on the crystallization kinetics of Cu–Zr [1–5] and Ni–Zr [6–9], those of Fe–Zr metallic glasses are relatively few, except those by some authors [10–15]. Buschow has investigated the crystallization kinetics of Fe–Zr metallic glasses both in the iron-rich and zirconium-rich regions [11]. Krebs *et al.* [12] have also reported the crystallization and structural studies of zirconium-rich Fe–Zr metallic glasses. But there are some discrepancies between their results. Furthermore, the details on the metastable phases precipitating during annealing still remain unresolved.

This work is one of the sequences of our studies on the crystallization kinetics of Fe–Zr metallic glasses. In a previous report, we have studied the crystallization of iron-rich Fe–Zr metallic glass, being concentrated on the effects of the surface crystalline layer [15]. In the present work we study the crystallization kinetics of zirconium-rich Fe–Zr metallic glasses in the concentration range 20 to 40 at % Fe by means of differential scanning calorimetry (DSC) and X-ray diffraction. The work on the crystallization kinetics of the sputtered Fe–Zr metallic glasses in the inter-

mediate region, from 25 to 55 at. % Fe, will be published in the future [16].

2. Experimental techniques

Alloys are prepared by arc-melting; electrolytic iron (99.8%) and sponge zirconium (99.8%) are arc-melted under titanium-gettered argon gas prior to melting together. All metallic glass samples are prepared by the melt-spinning method using copper-roll under argon gas atmosphere. The velocity of the roll surface is 62 m sec^{-1} . The amorphous structure of the fabricated samples is checked by X-ray diffraction with $\text{CuK}\alpha$ radiation.

Because zirconium is easily oxidized, the DSC apparatus (Rigaku, Thermoflex 8100) is evacuated up to $2 \times 10^{-3} \text{ Pa}$ prior to introducing 1 atm argon gas. But even under such condition, specimens cannot be prevented completely from oxidizing; traces of oxidation are sometimes detected by X-ray diffraction for the specimens after the DSC measurements. A heating rate of 15 K min^{-1} is adopted with a mass of 2 mg in the DSC measurements.

As-quenched ribbons are annealed both isothermally and isochronally in order to correlate the DSC results with those by X-ray diffraction. Isothermal annealing is carried out in a quartz tube which is evacuated up to $2.6 \times 10^{-4} \text{ Pa}$ prior to introducing 1 atm argon gas. Isochronal heating is carried out in the DSC apparatus in which specimens are annealed at a heating rate of 15 K min^{-1} and then cooled down by quickly removing them from the heating furnace.

3. Results

Fig. 1 is the results of DSC measurements showing the heat capacity change due to the crystallization for $\text{Fe}_x\text{Zr}_{100-x}$, $x = 20, 25, 30, 32, 35$ and 40, metallic

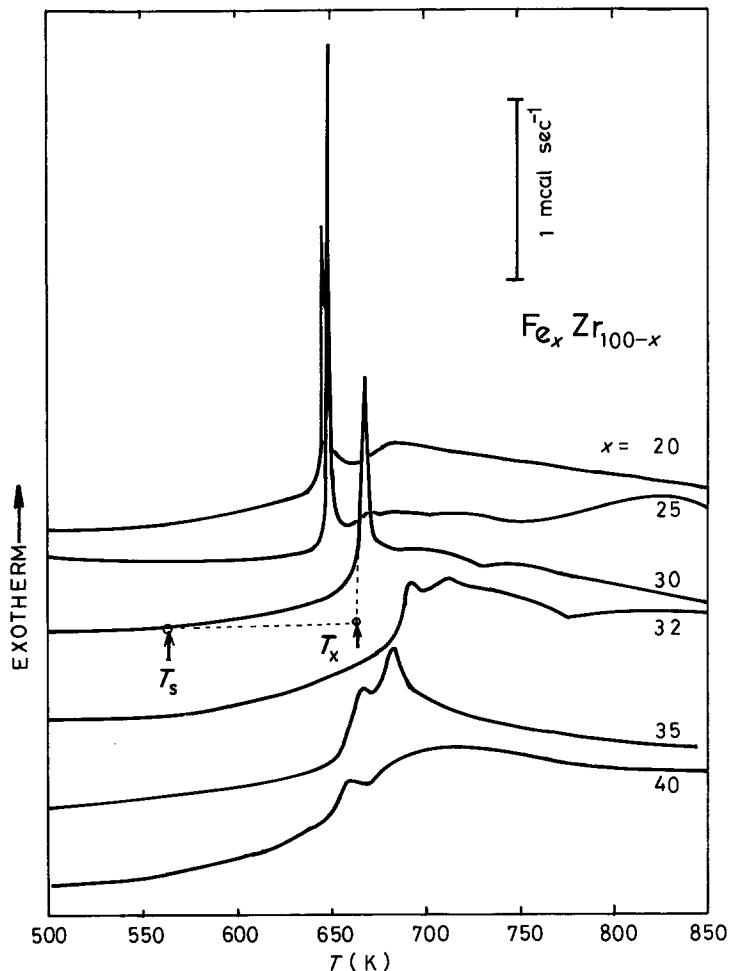


Figure 1 DSC curves for $\text{Fe}_x\text{Zr}_{100-x}$ metallic glasses with $x = 20, 25, 30, 32, 35$ and 40 at a heating rate of 15 K min^{-1} . The definitions of T_x and T_s are shown in the figure, where T_x is the onset temperature of crystallization, T_s the temperature at which DSC curve begins to show a gradual exotherm.

glasses. DSC curves for $20 \leq x \leq 30$ show a single and sharp exothermic peak denoting a high crystallization rate for these alloys. On the other hand, those for $32 \leq x \leq 40$ exhibit broad and composite exothermic peaks. Furthermore, those for $32 \leq x \leq 40$ exhibit slight and gradual exotherms below the onset temperature of crystallization.

Although the onset temperature of crystallization (T_x) cannot be determined unambiguously for the alloys which show the low-temperature exotherm, we define T_x in the manner as shown in Fig. 1. T_s is defined as the temperature where a DSC curve begins to deviate from a base line, as shown in Fig. 1. The concentration dependences of T_x and T_s are shown in Fig. 2 together with T_1 and T_2 , where T_1 and T_2 are the temperatures at the first and second exothermic peaks in the DSC curve, respectively. Although T_x , T_1 and T_2 do not depend much on the concentration, there is a broad maximum at around 32 at % Fe, which does not agree with the works by Krebs *et al.* [12] and Buschow [11]; Krebs *et al.* have reported the monotonic increase in T_x with iron and Buschow reported two maximum around 27 and 39 at % Fe. The source of such differences is not clear but it is probably because the glass formability decreases so much on approaching 40 at % Fe that preparation conditions, such as a cooling rate and an ambient gas, sensitively affects their crystallization kinetics. Alternatively, Fe-Zr metallic glasses, especially in the zirconium-rich region, are likely to be oxidized during DSC measurements, so an ambient gas may affect their thermograms.

The change in the X-ray diffraction patterns with annealing temperatures is shown in Fig. 3 for $\text{Fe}_{32}\text{Zr}_{68}$ as a typical example. The crystalline phase of this alloy that appears by annealing can be identified as a Ti_2Ni -type FeZr_2 compound, though some uncertainties still remain. Ti_2Ni -type FeZr_2 is known as an oxygen-stabilized intermetallic compound. Two types of the Ti_2Ni -type FeZr_2 have been reported [17, 18]:

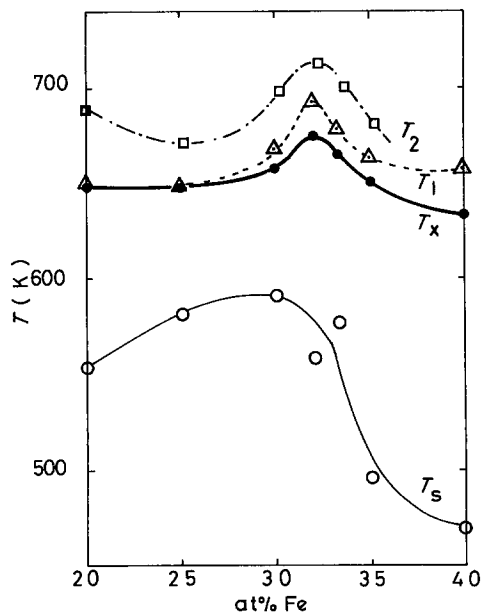


Figure 2 The concentration dependences of T_x , T_1 , T_2 and T_s determined from the DSC measurements with a heating rate of 15 K min^{-1} .

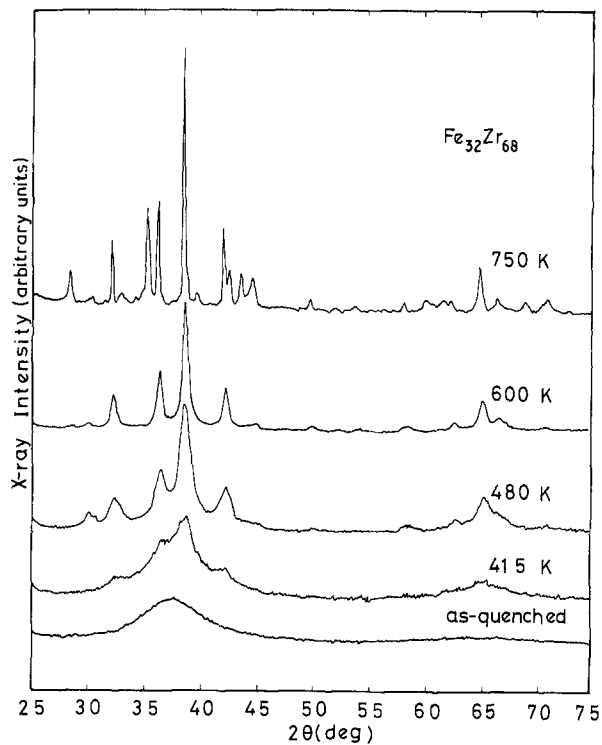


Figure 3 X-ray diffraction patterns of $\text{Fe}_{32}\text{Zr}_{68}$ metallic glass annealed at various temperatures for 15 min.

i.e. space groups of $\text{Fd}3\text{m}$ and $\text{Pm}3\text{m}$. The former, which is called $\text{Fe}_3\text{M}_3\text{C}$ -type, agrees with our X-ray data better than the latter. This type of crystalline phase will now be referred to as Ti_2Ni -type FeZr_2 .

Fig. 4 shows the X-ray diffraction data for $\text{Fe}_x\text{Zr}_{100-x}$, $x = 25, 30, 32$ and 35 , after annealing up to the temperature just above the first exothermic peak of the DSC curve, at a heating rate of 15 K min^{-1} . All the X-ray patterns for the alloys with $x \geq 30$ have similar reflection peaks which can be identified as Ti_2Ni -type FeZr_2 . On the other hand, the alloy with $x = 25$ has extra reflections which can be identified as $\omega\text{-Zr}$.

The crystalline phases determined by X-ray diffraction at respective annealing temperatures are sum-

marized in Fig. 5. In the lower iron region, $x = 20$ and 25 , $\omega\text{-Zr}$ and Ti_2Ni -type FeZr_2 appear simultaneously at the first crystallization step followed by the immediate transformation into orthorhombic FeZr_3 [19]. The $\text{Fe}_x\text{Zr}_{100-x}$ glasses with $x \geq 30$ crystallize into Ti_2Ni -type FeZr_2 which is stable up to our annealing temperatures. $\beta\text{-Zr}$ phase is ensured to appear for $x = 32$ and 33.3 above the temperature of 973 K .

These X-ray results are a little different from the phase diagram reported by Malakhova and Alekseyeva [19]; we cannot find Fe_2Zr and $\alpha\text{-Zr}$ for the alloys with $25 \leq x \leq 40$ and $20 \leq x \leq 25$, respectively, at 1020 K . It is probably because of the fairly short annealing time in our case (15 min) compared with their case (480 h).

4. Discussion

As described in the previous section, there are two kinds of crystallization modes for the $\text{Fe}_x\text{Zr}_{100-x}$, $20 \leq x \leq 40$, metallic glasses; the alloys with $20 \leq x \leq 25$ crystallize into $\omega\text{-Zr}$ and Ti_2Ni -type FeZr_2 with an accompanying single and sharp exothermic peak in the DSC curve, while the alloys with $32 \leq x \leq 40$ crystallize into Ti_2Ni -type FeZr_2 with accompanying broad and composite exothermic peaks.

Indeed crystallization of $\text{Fe}_{25}\text{Zr}_{75}$ glass takes place like an "explosive crystallization" [20]. On the other hand, the crystallization of the $\text{Fe}_x\text{Zr}_{100-x}$ glasses with $35 \leq x \leq 40$ occurs moderately. Furthermore, the DSC curves for these metallic glasses start to deviate from the base line showing a gradual exotherm in the lower temperature region. The $\text{Fe}_{30}\text{Zr}_{70}$ glass seems to be in an intermediate state between two crystallization modes described above; although the exothermic peak in the DSC curve shows a relatively sharp peak, the $\text{Fe}_{30}\text{Zr}_{70}$ glass also shows a gradual exotherm in a temperature below T_x .

This low-temperature exotherm observed for the alloys with $30 \leq x \leq 40$ below T_x does not induce the

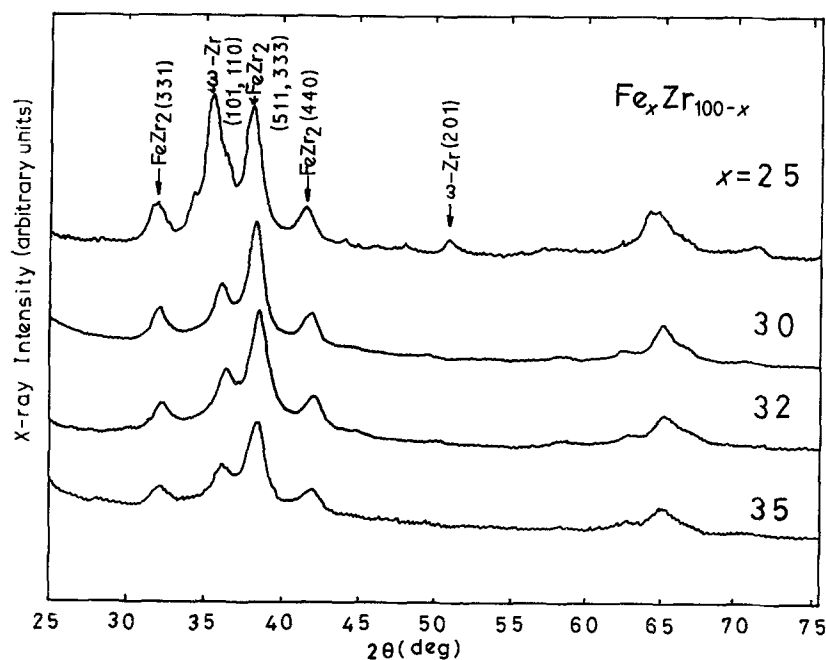


Figure 4 X-ray diffraction patterns for $\text{Fe}_x\text{Zr}_{100-x}$ metallic glasses with $x = 25, 30, 32$ and 35 after annealing up to just above the temperature of the first exothermic peak in the DSC curve with a constant heating rate 15 K min^{-1} .

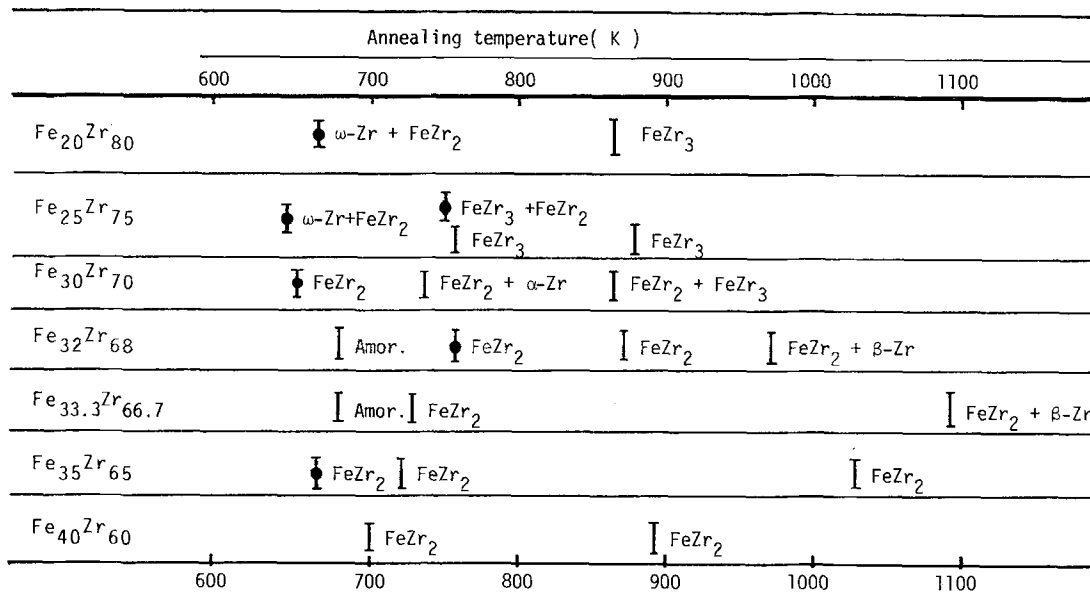


Figure 5 The crystalline phases appeared after annealing isothermally (⌈) and with a constant heating rate of 15 K min⁻¹ (⬇). These are identified by X-ray diffraction.

precipitation of crystallites visible to X-ray diffraction. For example, when the as-quenched $Fe_{32}Zr_{68}$ metallic glass is annealed for 100 min at 620 K, lower than T_x (675 K) but higher than T_s (558 K), the X-ray halo pattern for the annealed glass does not show any change. But the onset of the low-temperature exotherm is suppressed and the heat of the exotherm below T_x , as well as above T_x , decreases upon this annealing. Furthermore, as will be shown elsewhere [21], the intensity of the small-angle X-ray scattering increases significantly by annealing as-quenched $Fe_{30}Zr_{70}$ metallic glass at 575 K for 60 min, although the X-ray halo pattern is kept unchanged.

These facts suggest that the gradual exotherm observed for Fe_xZr_{100-x} metallic glasses with $30 \leq x \leq 40$ below T_x is induced by some atomic rearrangements which results in a decrease in the exothermic heat due to crystallization above T_x . Therefore, this gradual exotherm below T_x should be regarded as the precursor of crystallization or the early stage of crystallization.

This early stage crystallization observed for the alloys with $30 \leq x \leq 40$ may be associated with the fact that the glass formability in this concentration range decreases on going away from the eutectic point (24 at % Fe). The liquidus line of this alloy rises steeply with increasing iron content near the eutectic point, and it attains 1600 K at 40 at % Fe. Therefore, it is likely that the number of nuclei quenched-in during cooling from the melt increases with increasing iron content. The increase in the number of quenched-in nuclei may lead to an increase in the low-temperature exotherms for the alloys with $30 \leq x \leq 40$. The decreases in T_s and T_x with increasing iron content are also reflected on this fact.

Another possibility of the low and composite exotherm above T_x and low-temperature exotherm below T_x for the alloys with $30 \leq x \leq 40$ is that it is associated with the fact that Ti_2Ni -type $FeZr_2$ is stable only when it includes oxygen. So the low-temperature exotherm may reflect on the oxygen-penetrating

process into Fe-Zr amorphous matrix and the crystallization rate above T_x must be limited by the reaction rate between oxygen and the amorphous matrix.

In order to conclude the above work, more sophisticated experiments such as using transmission electron microscopy or Mössbauer spectroscopy are to be done. Furthermore, DSC measurement should be carried out under an ultra-high-vacuum in order to diminish completely the effects of oxygen on crystallization for zirconium-rich Fe-Zr metallic glasses.

When an amorphous alloy crystallizes into a single phase with the same composition as the amorphous matrix, it is called polymorphous crystallization [22, 23]. Since polymorphous crystallization does not need long range diffusion, the crystallization rate turns out to be high and so a single and sharp exothermic peak is usually observed at T_x ; for example, Fe_3B [24] and in some cases in Ni-Zr alloys [9]. Polymorphous crystallization can be expected to occur for the Fe_xZr_{100-x} , $20 \leq x \leq 40$, metallic glasses at the stoichiometric composition, e.g. $FeZr_2$, $FeZr_3$ and $FeZr_4$ etc.

It seems rather strange, however, that metastable $FeZr_3$ does not appear as the result of polymorphous crystallization, but $Fe_{25}Zr_{75}$ glass crystallizes in the most part to ω -Zr followed immediately by transition into $FeZr_3$ single phase.

The reason why $Fe_{25}Zr_{75}$ glass does not crystallize into $FeZr_3$ polymorphously may be as follows. Unless the cooling rate is enough to allow vitrification, a thin crystalline layer of ω -Zr is apt to be formed on the free surface (opposite to the roll-contacted side) of the melt-spun $Fe_{25}Zr_{75}$ and $Fe_{20}Zr_{80}$. This means that the nucleus or embryo of ω -Zr may be embedded in those amorphous matrices during vitrification. Therefore, crystallization of the $Fe_{25}Zr_{75}$ metallic glass should be triggered by the nucleus or embryo of ω -Zr and followed by its growth. This primary crystalline phase, ω -Zr, transforms into $FeZr_3$ single phase immediately, since the ω -Zr crystallite is super-saturated with iron which is unstable at a temperature above T_x .

5. Conclusion

Two different crystallization modes are found for the $\text{Fe}_x\text{Zr}_{100-x}$, $20 \leq x \leq 40$, metallic glasses. In the lower iron concentration region, $20 \leq x \leq 25$, Fe-Zr glasses crystallize into ω -Zr and Ti_2Ni -type FeZr_2 with an accompanying a sharp and large exothermic peak in the DSC curve. Immediately after crystallization, these crystalline phases transform into FeZr_3 with an accompanying slight exotherm. The alloys with $32 \leq x \leq 40$ crystallize into Ti_2Ni -type FeZr_2 at a low crystallization rate with an accompanying moderate exotherm. The $\text{Fe}_{30}\text{Zr}_{70}$ metallic glass seems to be situated at the intermediate state between two different crystalline modes. The alloys with $30 \leq x \leq 40$ exhibit a gradual exotherm from a temperature far below T_x . This low-temperature exotherm observed in the higher iron concentration region seems to be associated with the quenched-in nucleus or embryo. As the glass formability decreases with increasing iron content, the quenched-in nucleus or embryo, which may be invisible to X-ray diffraction, is likely to be formed in an amorphous matrix during the vitrification process. These quenched-in nuclei or embryos significantly affect the crystallization kinetics of these metallic glasses.

We conclude that the crystallization kinetics of $\text{Fe}_x\text{Zr}_{100-x}$, $20 \leq x \leq 40$ metallic glasses must be affected significantly by the solidification process such as cooling rate and sample preparing method.

Acknowledgement

I would like to thank Mr F. Takahashi for preparing the parent alloys by arc-melting.

References

1. R. L. FREED and J. B. VANDER SANDE, *J. Non-Cryst. Solids* **27** (1978) 9.
2. A. J. KERN, D. E. POLK, R. RAY and B. C. GIESSEN, *Mater. Sci. Eng.* **38** (1979) 49.
3. K. H. J. BUSCHOW, *J. Appl. Phys.* **52** (1981) 3319.
4. J. M. VITEK, J. B. VANDER SANDE and N. J. GRANT, *Acta Metall.* **23** (1975) 165.
5. Z. ALTOUNIAN, Tu GUO-HUA and J. O. STORM-OLSEN, *J. Appl. Phys.* **53** (1982) 4755.
6. K. H. J. BUSCHOW and N. M. BEEKMANS, *Phys. Rev.* **B19** (1979) 3843.
7. M. NOSE and T. MASUMOTO, *Sci. Rep. Ins. Tohoku Univ. Ser. A28* (1980) 232.
8. D. DONG, G. GREGAN and M. G. SCOTT, *J. Non-Cryst. Solids* **43** (1981) 403.
9. Z. ALTOUNIAN, Tu GUO-HUA and J. O. STORM-OLSEN, *J. Appl. Phys.* **54** (1983) 3111.
10. I. VINCZE, F. Van der WOUDE and M. G. SCOTT, *Solid State Commun.* **37** (1981) 567.
11. K. H. J. BUSCHOW *J. Phys. F Met. Phys.* **14** (1984) 593.
12. H. U. KREBS, C. MICHAELSEN, J. REICHELDT, H. A. WAGNER, J. WECKER, Q. R. ZHANG and H. C. FREYHARDT, *J. Non-Cryst. Solids.* **61/62** (1984) 463.
13. M. SOSTARICH and Y. KHAN, *Z. Metallkde* **73** (1983) 706.
14. K. OSAMURA, S. OCHIAI and S. TAKAYAMA, *J. Mater. Sci.* **19** (1984) 1917.
15. M. MATSUURA, *J. Phys. F Met. Phys.* **15** (1985) 257.
16. *Idem*, to be published.
17. M. V. NEVITT, J. W. DOWNEY R. A. MORRIS, *Trans. Met. Soc. AIME* **218** (1960) 1019.
18. B. KUŽMA, V. Y. MARKIV, Y. V. VOROSHILOV and R. V. SKOLOZRA, *Inorg. Mater.* **2** (1966) 222.
19. T. O. MALAKHOVA and Z. M. ALEKSEYEVA, *J. Less-Common Metals* **81** (1981) 293.
20. A. GÖTZBERGER, *Z. Phys.* **142** (1955) 182.
21. M. MATSUURA, to be published.
22. U. KÖSTER and U. HEROLD, "Glassy Metals I", edited by H.-J. Güntherodt and H. Beck (Springer Verlag, Berlin, 1981) p. 225.
23. M. G. SCOTT, "Amorphous Metallic Alloys", edited by F. E. Luborsky (Butterworths, London, 1983) p. 144.
24. U. HEROLD and U. KÖSTER, in Proceedings of the 3rd International Conference on Rapidly Quenched Metals, Vol. 3, Brighton, August (1977) edited by B. Cantor (The Metal Society, London, 1978) p. 281.

Received 15 July

and accepted 13 September 1985